6-2005

Manganese Distribution across the Blood-Brain Barrier. IV. Evidence for Brain Influx through Store-Operated Calcium Channels

Janelle S. Crossgrove
University of Kentucky

Robert A. Yokel
University of Kentucky, ryokel@email.uky.edu

Manganese Distribution across the Blood-Brain Barrier. IV. Evidence for Brain Influx through Store-Operated Calcium Channels

Digital Object Identifier (DOI)
https://doi.org/10.1016/j.neuro.2004.09.004

Notes/Citation Information
Published in *Neurotoxicology*, v. 26, issue 3.

MANGANESE DISTRIBUTION ACROSS THE BLOOD-BRAIN BARRIER

IV. EVIDENCE FOR BRAIN INFLUX THROUGH STORE-OPERATED CALCIUM CHANNELS

Janelle S. Crossgrove[1,2] and Robert Yokel[1,3]

[1]Graduate Center for Toxicology, University of Kentucky Medical Center, Lexington, KY, 40536-0305, [2]Present address: School of Health Sciences, Purdue University, West Lafayette, IN, 47907 and [3]College of Pharmacy, University of Kentucky Medical Center, Lexington, KY, 40536-0082.

Robert Yokel

511C Pharmacy Building

University of Kentucky

907 Rose Street

Lexington, KY 40536-0082

Phone: (859) 257-4855

Fax: (859) 323-6886

E-mail: ryokel@email.uky.edu

ABSTRACT

Manganese (Mn) is a required co-factor for many ubiquitous enzymes; however, chronic manganese overexposure can cause manganism, a parkinsonian-like syndrome. Previous studies showed manganese influx into brain is carrier-mediated, though the putative carrier(s) were not established. Studies conducted with cultured bovine brain microvascular endothelial cells (bBMECs), which comprise the blood-brain barrier, revealed ^{54}Mn (II) uptake positively correlated with pH, was temperature-dependent, and was sodium- and energy-independent. Brain ^{54}Mn uptake correlated inversely with calcium (Ca) concentration, but ^{45}Ca uptake was unaltered by high Mn concentration. Lanthanum (La), a non-selective inhibitor of several Ca channel types, as well as verapamil and amiloride, inhibitors of voltage-operated Ca channels, failed to inhibit Mn uptake into cells. Nickel (Ni), another non-selective inhibitor of several Ca channel types, inhibited Mn and Ca uptake into cells by 88 and 85 %, respectively. Cyclopiazonic acid (CPA) and thapsigargin, which activate store-operated calcium channels (SOCCs), increased ^{54}Mn and ^{45}Ca uptake into cultured bBMECs. *In situ* brain perfusion studies were conducted in adult, male Sprague-Dawley rats to verify the cell culture results. Both nickel and verapamil produced a non-significant decrease in Mn and Ca influx. Lanthanum significantly increased Mn influx to 675 and 450 % of control in parietal cortex and caudate, respectively, while producing no significant effect on Ca influx. Vanadate, which inhibits Ca-ATPase, inhibited Mne uptake into cultured blood-brain barrier cells, but not into perfused rat brain. Overall these results suggest that both Ca-dependent and Ca-independent mechanisms play a role in brain Mn influx. This work provides

evidence that store-operated Ca channels, as well as another blood-brain barrier transporter, are likely to mediate carrier-mediated Mn influx into the brain.

Running title: Mn brain influx at the BBB through SOCs

Key words/phrases: manganese, blood-brain barrier, influx, store-operated calcium channel

INTRODUCTION

The trace element manganese (Mn) is essential for normal brain development and function throughout the life span of all mammals (Keen *et al.*, 2000). Mn is a co-factor for many enzymes, including the brain-specific enzyme glutamine synthetase (Wedler and Denman, 1984) and ubiquitously expressed enzymes including superoxide dismutase 2 and pyruvate carboxylase (Keen*, et al.*, 2000). While Mn is essential for normal brain function, excess brain Mn is neurotoxic and can produce manganism, a parkinsonian-like syndrome (Hudnell, 1999; Iregren, 1999). Neurotoxicity due to excess Mn has been reported following occupational inhalation exposure to Mn in mining operations (Couper, 1837), in dry-cell battery production (Keen and Lönnerdal, 1995), in ferromanganese smelting (Huang *et al.*, 1989) and during Mn welding operations (Chandra *et al.*, 1981; Ono *et al.*, 2002); following non-occupational exposure to inhaled Mn (Hudnell, 1999) and following intestinal exposure of Mn in drinking water. There is currently significant concern about airborne Mn exposure from the fuel additive methylcyclopentadienyl manganese tricarbonyl (MMT) (Hudnell, 1999). Current treatments for patients with manganism may postpone the progression of symptoms, but have not been able to cure the disease (reviewed in (Lee, 2000).

As the general public's Mn exposure increases with increased MMT use, the mechanisms of Mn homeostasis become more important in understanding and assessing the risk of neurotoxicity. Mn brain entry from blood can occur through the capillary endothelial cells of the blood-brain barrier (BBB) and through the choroid

plexuses. Several studies suggested that Mn ion brain influx at the BBB is carrier-mediated (Aschner and Aschner, 1990; Murphy *et al.*, 1991; Rabin *et al.*, 1993; Aschner and Gannon, 1994; Crossgrove *et al.*, 2003). Similarly, Mn appears to be actively transported into bile, achieving a concentration gradient as high as 100-fold (Klaassen, 1974). The identity of the Mn carrier(s) is unknown. Mn efflux across the BBB does not appear to occur through a carrier but rather by diffusion (Yokel *et al.*, 2003). Several studies suggested that the divalent metal transporter-1 (DMT-1) may be responsible for Mn ion influx into brain (Goddard *et al.*, 1997; Gunshin *et al.*, 1997; Conrad *et al.*, 2000), but a recent report suggests that the lack of functional DMT-1 in rats has no effect on brain influx of the Mn ion or the Mn-transferrin complex (Crossgrove and Yokel, 2004).

The current work examined whether brain Mn influx at the BBB is mediated by one or more calcium (Ca) transport pathways. Ca inhibited Mn entry into Hep-G2 cells (Finley, 1998). Cell Mn entry across cell membranes was decreased by Ca inhibitors (Mason *et al.*, 1993) and increased by activators of Ca influx (Kerper and Hinkle, 1997a). Mn entry through store-operated Ca channels (SOCs) has been demonstrated in rat mast and osteoblast-like cells and human platelets (Fasolato *et al.*, 1993; Dobrydneva and Blackmore, 2001; Baldi *et al.*, 2002). Others have reported evidence of SOCs on brain endothelial cells (Kerper and Hinkle, 1997b; Kim *et al.*, 2004). In this work, we examined the mechanism(s) of Mn brain entry across the BBB. We first examined general characteristics of Mn uptake at the BBB

and then tested the hypothesis that Mn influx at the BBB occurs through one or more Ca influx processes.

MATERIALS AND METHODS

Materials

$^{54}MnCl_2$ (specific activity 107 or 38 nCi/ng; total Mn 184 or 477 nM) in 0.5 M HCl was purchased from Perkin-Elmer/NEN (Boston, MA). $^{45}CaCl_2$ (5.87 nCi/ng) in water was purchased from Perkin-Elmer/NEN. [^{14}C]sucrose was purchased dry from Perkin-Elmer/NEN (3.6 nCi/nmol) and in 2% ethanol from Moravek (Brea, CA; 495 nCi/nmol) or American Radiolabeled Chemicals, Inc. (620 nCi/nmol). All other chemicals were purchased from Sigma (St. Louis, MO) unless otherwise noted. Sprague-Dawley rats (225-300 g) were purchased from Harlan (Indianapolis, IN). Verapamil was solubilized in methanol, diluted and delivered in 0.2% methanol. Thapsigargin was solubilized by DMSO and cyclopiazonic acid by methanol and delivered in 0.1% DMSO or methanol. Vehicle controls contained equimolar solvent. All animal research was conducted under the guidelines of the Guide for the Care and Use of Laboratory Animals and with the approval of the University of Kentucky Institutional Animal Care and Use Committee.

Isolation of bovine brain microvascular endothelial cells (bBMECs)

The bBMECs were isolated from fresh bovine brains, as described (Bowman *et al.*, 1983; Audus *et al.*, 1996). Cells were grown in 35 mm plastic dishes at 37°C in 5% CO_2 with nutrient media containing 10% horse serum in 50% MEM and 50% Ham's

F-12 supplemented with $NaHCO_3$ (13 mM), HEPES (10 mM) penicillin G (100 U/mL) and streptomycin (100 μg/ml). Cell identity was verified by the presence of the following characteristics of bBMECs. 1.) They were positive for γ-glutamyltransferase and alkaline phosphatase activity. 2.) They did not have the processes or shapes of neurons or glial cells according to morphologic analysis of TEM images. 3.) They took up histidine (Yamakami *et al.*, 1998).

Studies of ^{54}Mn uptake conducted in bBMECs

^{54}Mn uptake was determined in 85-90% confluent cell cultures following procedures established for another BBB cell line (Yokel *et al.*, 2002). In summary, each cell-containing culture dish was rinsed three times with a wash solution containing (in mM): Na^+ 122, K^+ 4.2, Ca^{2+} 1.5, Mg^{2+} 0.9, Cl^- 131, HEPES 10, and D-glucose 10 at pH 7.4 and at the temperature of the uptake experiment. The last wash remained in the dish at least 10 minutes to bring the cells to the temperature of the uptake experiment. The cells were incubated with 0.75 mL uptake solution consisting of wash solution containing $^{54}Mn^{2+}$ (~1 μCi/mL) and [^{14}C]-sucrose (1 μCi/mL; 0.2 μM) in the presence or absence of treatment. After 10 to 120 minutes the uptake solution was removed and the cells rapidly washed 5 times with ice-cold wash solution. Cells were solubilized in 1 M sodium hydroxide for 15 min at room temperature then neutralized with equimolar HCl. Aliquots of cell lysates were collected for analysis of radioactivity and total protein content.

Cell viability was measured in parallel dishes of cultured bBMECs exposed to the same treatments in the absence of the radionuclides. Cell membrane integrity was measured by determining the activity of the cytosolic enzyme lactate dehydrogenase (LDH) released into the uptake media. LDH activity was measured with an assay kit (Sigma). Cell redox potential, an indicator of cell health, was measured by methylthiazoletetrazolium (MTT) conversion to its formazan product. When MTT conversion was less than 80% of control the cells were considered to have drastically changed. Data from these cells were not used (except in studies of metabolic inhibitors and low temperature).

bBMECs were selected as a model of the BBB to screen characteristics of Mn uptake, with the intent of following significant findings in the intact rat. Initially, Mn uptake into bBMECs was measured from 10-120 minutes at pH 6.4 and 7.4 to determine whether it was linear, as several pHs were used in subsequent studies. $^{54}Mn^{2+}$ uptake over 30 minutes was measured in media buffered to pH 5.4, 6.4, 6.9, 7.4 and 7.9 by 10 mM potassium hydrogen phthalate (pH 5.4), PIPES (pH 6.4), MOPS (pH 6.9), or HEPES (pH 7.4 and 7.9). Mn uptake was also measured during a 30 minute incubation at 4 (on ice), 8, 21, 30 and 37°C; at 37°C in the presence of a metabolic inhibitor, 2,4-dinitrophenol (0.25 mM) or azide (10 mM); and with the replacement of glucose (10 mM) by 2-deoxyglucose (10 mM). The role of sodium in Mn uptake was measured by replacing 50 or 100% of the sodium in the uptake media with choline or lithium or by the addition of ouabain (0.1 mM). The role of Ca transporters in Mn uptake was examined by changing Ca concentration from 0 to 1.5 mM; by addition

of Ca transporter inhibitors including vanadate (0, 0.003, or 1 mM), lanthanum (La^{3+}; 0.050 mM as $La(NO_3)_3$), nickel (Ni; 1 mM as $NiCl_2$) or verapamil (0.3 mM); or by addition of the Ca transporter activators cyclopiazonic acid (CPA; 0.01 mM) and thapsigargin (0.001 mM).

In situ brain perfusion studies

Rats were prepared and perfused as described previously (Crossgrove*, et al.*, 2003). Briefly, a cannula containing heparinized saline was inserted into the right common carotid artery. The open end was transferred to a syringe containing a perfusate with the treatment and/or radioisotope tracers. Perfusate delivery was regulated by a syringe pump. Immediately before brain perfusion began, the rat's cardiac ventricles were severed to avoid mixing of blood with perfusate. The perfusion (45, 90 or 180 s) was terminated by decapitation. The brain was extracted and the ipsilateral parietal cortex, caudate and lateral ventricular choroid plexus removed, weighed and assayed for radioactivity. In some experiments, the cerebrum was homogenized according to the capillary depletion method as described (Crossgrove*, et al.*, 2003).

The perfusate contained 1 to 2 μCi $^{54}Mn^{2+}$/ml and a marker for vascular and extracellular space, ^{14}C-sucrose (1 μCi/ml), in a solution containing (in mM): Na^+ 122, K^+ 4.2, Ca^{2+} 1.5, Mg^{2+} 0.9, Cl^- 131, glucose 10, and HEPES 10. To test the hypothesis that Mn and Ca share one or more transporters, rats were treated with perfusates containing $^{54}Mn^{2+}$ and 0 added, 1.5 (control) or 9 mM Ca or ^{45}Ca and Mn (0 or 15 mM). Other experiments included the Ca transporter inhibitors sodium

vanadate (1 or 10 mM), *p*-hydroxyhippuric acid (0.4 mM), verapamil (0.3 mM) or amiloride (0.84 mM) to determine whether Ca transporters play a role in rat brain Mn influx.

Radioactivity and total protein determination

Radioactivity of ^{54}Mn and ^{14}C were determined in aliquots of cell lysate or in digested tissue as described (Crossgrove*, et al.*, 2003). Radioactivity from ^{45}Ca was counted from 156-257 keV by a liquid scintillation counter, with appropriate corrections for crossover, quench and decreased efficiency due to the narrowed counting window. Protein concentration in cell lysates was measured via the bicinchoninic acid method with a kit (Sigma).

Data and statistical analysis

In bBMEC experiments, ^{54}Mn, ^{45}Ca and ^{14}C activities (dpm/dish) and total protein (mg/dish) were calculated. ^{54}Mn, ^{45}Ca and [^{14}C]-sucrose uptake values were converted to dpm/mg protein. Non-specific binding to cell and collagen surfaces was determined by apparent uptake in 15 s on ice. Collagen was found to sequester Mn, but not ^{14}C or ^{45}Ca, during the time course of these experiments. Estimated confluence was used to predict the surface area of the collagen-coated dish that was exposed to ^{54}Mn uptake media. Uptake into collagen was determined as:

Mn uptake into collagen = (100%-confluence%)*(uptake into collagen-only dish)

Nonspecific Mn adsorption to the dish was also determined several times. It was negligible. Non-specific binding and estimated binding to collagen were subtracted from total uptake to obtain corrected values for ^{54}Mn, ^{45}Ca, and ^{14}C uptake into cells. These corrected values (dpm/mg protein) were divided by the activity of the uptake solution (dpm/ml) to obtain a volume of distribution of uptake (ml/mg protein) from uptake media.

The [^{14}C]-sucrose volume represents diffusional and pinocytotic uptake processes. This value was subtracted from the ^{54}Mn and ^{45}Ca volumes of distribution to generate a term expressing Mn or Ca uptake into the cells via carrier(s). Mn uptake (ml/mg protein) was converted to pmol Mn/mg protein by multiplying by total Mn concentration. Intracellular Mn concentration was then estimated from the relationship of 2 μl intracellular space per mg total protein (Edlund and Halestrap, 1988; Poole *et al.*, 1989).

In perfusion experiments, radioactivity (dpm/g tissue) was divided by perfusate activity (dpm/ml) to calculate the volume of distribution (ml/g). This was divided by the perfusion duration (45 to 90 s) to obtain the influx transfer coefficient (K_{in}), as described in detail (Crossgrove*, et al.*, 2003). All bBMEC experiments were completed with at least three replicates per experiment, each conducted in duplicate or triplicate. Results of the time course of Mn uptake at pH 6.4 and 7.4 were analyzed by regression analysis using GraphPad Prism to determine if uptake was best fit by a first or second order relationship. Uptake in the presence of treatments

was converted to a percent of control uptake for each experiment. The mean and relative standard deviation were calculated. For cell and perfusion experiments, t-tests or one-way ANOVAs were conducted using GraphPad Prism to test for treatment differences. When treatment differences were found, post-hoc comparisons by Dunnett's or Bonferroni's tests were conducted after the ANOVAs to determine significant differences among treatment groups.

For all studies, $p < 0.05$ was accepted as statistically significant.

RESULTS

^{54}Mn uptake into bBMECs was initially studied up to 120 minutes to assess linearity during that time (Figure 1 *Inset*). Regression analysis showed Mn uptake results obtained at pH 7.4 and 6.4 were better fit by linear than non-linear regression. The 95% confidence intervals for the slopes excluded one another. Mn^{2+} uptake at pH 6.4 was significantly less than at 7.4. For the remaining studies, 30-minute uptake was used as representative.

At the 120 minute time point, the intracellular Mn concentration (overall means of 10.6 and 3.4 μM for pH 7.4 and 6.4, respectively), exceeded the media Mn concentration (184 nM) by at least 10 fold. In later experiments using ^{54}Mn at a lower specific activity and higher total Mn (477 vs. 184 nM), the intracellular concentration at 30 minutes was at least 3-fold, and usually 10-fold, greater than the extracellular

concentration. Intracellular Mn concentration was higher than extracellular Mn concentration in all experiments under control conditions.

Mn uptake was inversely related to proton concentration. This was noted in the time course of Mn uptake conducted at pH 6.4 and 7.4 as well as the uptake study conducted at pH 5.4, 6.4, 6.9, 7.4 and 7.9 (Figure 1). The results from cells treated at pH 5.4 for 30 minutes are not shown because they produced only 6% of the formazan product/mg protein that was found in control (pH 7.4) cells, indicating severe cell toxicity.

Temperature-dependence of uptake

Mn uptake into bBMECs was measured at five temperatures. The data were graphed as an Arrhenius plot of natural log of the uptake rate versus inverse of absolute temperature (Figure 2). The plot appears to have a change in slope (a breakpoint); however, the data are not significantly non-linear. Rearrangement of the Arrhenius equation, as follows, generated the activation energy (E_a).

$$E_a = -R * (d \ln k)/d (1/T)$$

where R is the ideal gas constant, k is the uptake rate and $d(\ln k)/d(1/T)$ is the slope of Figure 2. E_a was determined to be 27 kJ/mol.

Sodium- and energy-independence of uptake

Mn uptake into bBMECs was not inhibited by replacement of the sodium in the uptake medium (Table 1). Sodium replacement by choline resulted in a significant increase of Mn uptake into bBMECs. Energy production inhibitors reduced MTT conversion to formazan by ~ 40% (results not shown) but did not significantly affect Mn uptake into bBMECs (Table 1).

Calcium-dependence of bBMEC uptake and brain influx

There was an inverse relationship between Ca concentration and brain Mn influx (Figure 3) as well as Mn uptake and Ca concentration in bBMECs (Table 2). However, Mn did not inhibit brain Ca influx (Figure 3).

La^{3+} increased brain Mn influx (Figure 4), and Ni did not decrease Mn influx into rat brain (Figure 5). Verapamil did not significantly inhibit Mn influx compared to control. Mean Mn influx values ± SEM (n=5-6) for control versus verapamil were 20.6 ± 2.7 vs. 14.9 ± 1.6; 12.4 ± 2.5 vs. 6.6 ± 0.4; and 1218 ± 108 vs. 863 ± 62 x 10^{-5} ml/s/g for parietal cortex, caudate or choroid plexus, respectively. Another voltage-gated Ca channel inhibitor, amiloride, did not inhibit brain Mn influx (Ca was not tested). Mn influx values for control versus amiloride-treated brains were 6.2 ± 2.2 vs. 11.3 ± 5.7; 6.7 ± 0.7 vs. 4.7 ± 1.6; 2197 ± 421 vs. 1756 ± 178 x 10^{-5} ml/s/g for the parietal cortex, caudate or choroid plexus, respectively (mean ± SEM of 4 control and 3 treated brains).

Brain Ca influx was measured concurrently with Mn influx for control perfusates and those with La, Ni or verapamil. Control Ca influx values (mean ± SEM, n=5-6) were 85.1 ± 15.7, 61.4 ± 11 and 873 ± 177 x 10^{-5} ml/s/g for parietal cortex, caudate and choroid plexus, respectively. Ca influxes with La were 75 ± 22.9, 55.1 ± 27.2 and 672 ± 145 x 10^{-5} ml/s/g. Ca influx with Ni were 62.1 ± 18.5; 39.6 ± 10; and 1058 ± 497 x 10^{-5} ml/s/g for parietal cortex, caudate and choroid plexus, respectively; with verapamil, 80.4 ± 10.5; 54.7 ± 7.5; and 922 ± 182 x 10^{-5} ml/s/g. Brain Ca influx was not significantly affected by any of these treatments within this short time course.

La^{3+} decreased Ca uptake into bBMECs without having a significant effect on Mn uptake (Table 2). Ni significantly inhibited Ca and Mn uptake into bBMECs (Table 2). In addition to its effect on brain influx, verapamil also produced parallel, non-significant decreases of Mn and Ca uptake into bBMECs (Table 2).

Vanadate (1 mM) did not significantly inhibit Mn influx into the tested brain regions or the choroid plexus following its co-perfusion with $^{54}Mn^{2+}$ for 90 seconds. Mean values ± SEM (4 rats per group) were 49.2 ± 21.1 vs. 51.2 ± 23.8, 7.4 ± 2.8 vs. 17.0 ± 10.5 and 759 ± 347 vs. 450 ± 190 x 10^{-5} ml/s/g for control vs. vanadate-treated parietal cortex, caudate and choroid plexus tissues. When the brain was perfused with 1 mM vanadate for 90 s and then immediately switched to a co-perfusion of vanadate with $^{54}Mn^{2+}$, Mn influx was not inhibited by the vanadate pre-wash exposure. The control and vanadate-treated brain Mn influx values were 4.4 ± 0.9

vs. 16.4 ± 7.7, 2.6 ± 0.7 vs. 4.0 ± 0.7 and 247 ± 35 vs. 746 ± 53 x 10^{-5} ml/s/g for the parietal cortex, caudate and choroid plexus regions of the brain, respectively (mean ± SEM for 6 rats per group). A higher concentration of vanadate (10 mM) also failed to inhibit brain Mn influx. The parietal cortex, caudate and choroid plexus Mn influx values were 13.4 ± 4.4 vs. 21.5 ± 6.6, 7.4 ± 1.6 vs. 11.4 ± 4.1 and 1063 ± 294 vs. 1376 ± 318 x 10^{-5} ml/s/g brain for control vs. vanadate-treated brain, respectively (mean ± SEM for 5 rats per group). Vanadate did not change the distribution of Mn in the endothelial cells or the brain parenchyma. Endothelial cells retained 10 and 13% of the total Mn entering brain following perfusion with Mn or Mn with vanadate (10 mM; data not shown). Therefore, brain parenchyma contained 90 and 87% of the Mn that had crossed the BBB.

Contrary to *in situ* perfusion results, addition of 3 μM or 1 mM vanadate inhibited Mn uptake into bBMECs (Table 2). Furthermore, this effect persisted after vanadate was washed out. Cells treated 30 minutes with 1 mM vanadate, washed twice and incubated with vanadate-free uptake media had only 39% of control Mn uptake (Table 2).

Addition of *p*-hydroxyhippuric acid (0.4 mM) to the brain perfusate did not inhibit brain Mn influx (Ca influx was not tested). The control and experimental brain Mn influx values were 7.4 ± 0.6 vs. 12.7 ± 1.8, 8.6 ± 1.4 vs. 6.7 ± 0.6 and 1375 ± 100 vs. 1310 ± 122 x 10^{-5} ml/s/g for the parietal cortex, caudate and choroid plexus, respectively (mean ± SEM for 6 control and 7 treated rats). In the cerebellum only,

there was a non-significant trend for a *p*-hydroxyhippuric acid-induced decrease of Mn influx (11.0 ± 1.9 vs. 5.7 ± 0.6 x 10^{-5} ml/s/g for control vs. *p*-hydroxyhippurate).

Studies with modulators of store-operated Ca channels

CPA significantly increased Mn and Ca uptake when studied concurrently (Table 2). Ca uptake following thapsigargin treatment was not significantly greater than control (*P*=0.07), although Ca uptake in thapsigargin-treated cells was 1.4-10 fold greater than in control cells in each experimental replicate. Mn uptake was significantly greater in thapsigargin-treated than in control cells (Table 2).

DISCUSSION

This research examined the mechanism of carrier-mediated Mn entry into the rat brain across the BBB. The first objective was to determine general characteristics of carrier-mediated Mn uptake. The second objective tested the hypothesis that brain Mn entry was mediated by one or more Ca transporters. The results suggest that brain Mn influx occurs through at least one pathway which is not Ca-mediated as well as one or more pathways involving SOCs.

Our results are consistent with previous reports of carrier-mediated Mn uptake at the BBB (Aschner and Aschner, 1990; Murphy*, et al.*, 1991; Rabin*, et al.*, 1993; Aschner and Gannon, 1994; Crossgrove*, et al.*, 2003). Here, we report concentrative Mn uptake, providing evidence of a carrier-mediated process. The temperature-dependence study suggests that the activation energy of this process is 27 kJ/mol, consistent with values reported for ion channels (18-34 kJ/mol) by

electrophysiological techniques (Liu et al, 1996). This supports the suggestion that brain Mn uptake occurs through one or more carrier-mediated processes. Finally, the negative correlation between proton concentration and Mn uptake into bBMECs agrees with our report that Mn uptake is not likely to occur through the divalent metal transporter-1, which co-transports a proton with a divalent metal ion (Crossgrove and Yokel, 2004).

Brain Mn uptake was not inhibited by 2,4-dinitrophenol, azide or 2-deoxyglucose, suggesting it is not directly dependent on an energy source mediated by ATP hydrolysis. Nor was brain Mn uptake inhibited by ouabain, showing it to be independent of Na^+/K^+-ATPase. While these studies did not provide evidence for energy dependence, the concentrative uptake seen in the bBMEC studies must rely on an energy source or electron transfer. The conversion of MTT to formazan in treated cells was ~60% of control cells, suggesting reduction, but not elimination, of cell redox potential when ATP-inhibitors were present. Therefore, the lack of effect by metabolic inhibitors may be due either to the lack of an ATP-dependent Mn transporter or to the ability of the ATP-dependent Mn transporter(s) to continue at their normal rate when ATP is reduced to 60%. Alternatively, the pH dependence suggests that there might be an electromotive driving force maintaining Mn uptake. However, the positive correlation between Mn uptake and pH suggest that it is not an inward proton or cation electromotive force. This suggests that the Mn transporter may be a proton or cation antiporter.

Brain Mn uptake was sodium-independent, suggesting the uptake carrier(s) do not utilize a sodium gradient as a driving force. Replacing sodium with choline increased brain Mn uptake. One report provides evidence that Mn inhibits choline uptake at the BBB (Lockman *et al.*, 2001). The authors suggested that the choline transporter may be involved in brain Mn uptake, though they did not test the effect of choline on Mn uptake. Choline uptake into rat brain, like Mn uptake, has been described to be sodium-independent (Allen and Smith, 2001). Mn and choline may share one or more transport process(es). On the other hand, choline increased Mn uptake, which would not be expected if they were competing for an uptake process. While the basis of any interaction between Mn and choline is unclear, it is clear that Mn uptake at the BBB is sodium independent.

Ca appears to play a significant role in Mn influx at the BBB. When Ca was not added to the perfusate, Mn influx was significantly greater than in the presence of normal (1.5 mM) Ca. Brain Mn influx was slightly, but not significantly, less in the presence of 9 mM Ca. Ca has been shown to inhibit Mn uptake into astrocytes in competitive and non-competitive manners (Aschner *et al.*, 1992). Mn uptake into bBMECs also increased in the absence of added Ca compared to uptake media with normal (1.5 mM) Ca. Overall, Ca concentration correlates negatively with Mn influx. This concentration-dependent effect does not distinguish whether Ca and Mn directly compete for the same carrier or whether Ca indirectly modulates Mn uptake. On the other hand, added Mn did not inhibit ^{45}Ca influx into rat brain compared to control (no added Mn) perfusate (Figure 3), suggesting Mn and Ca do not compete

for the same carrier, or that the capacity of any common carrier(s) is very large. Depending on the affinity of the Ca carrier for Mn, the 10-fold greater concentration of Mn above that of Ca used in the present studies may not be sufficient to inhibit brain Ca influx. A 6-fold increase in Ca failed to significantly inhibit Mn influx, which suggests either that they have separate carriers or that their shared pathway(s) has a great substrate capacity.

Mn uptake into bBMECs was inhibited by Ni, consistent with a role for Ca channels in Mn uptake. Ni has been shown to inhibit receptor-operated Ca channels and store-operated channels (Cui and Dannies, 1992; Kukkonen *et al.*, 2001). Ni is thought to be a rather specific inhibitor of Ca channels, as it did not appear to be a substrate for the channels it blocks (Shibuya and Douglas, 1992; Jones and Sharpe, 1994). In the current study, Ni blocked Mn uptake (to 12% control) in bBMECs in a manner parallel to its effect on Ca uptake (15% control), providing strong evidence that Mn uptake may occur through Ca uptake pathways. An alternative explanation is that Ni blocks equally two or more separate pathways for Mn and Ca uptake, rather than our suggestion of a common pathway. In perfusion studies, Ni failed to block Mn and Ca brain influx. The difference between the animal and bBMEC studies may be due to the shorter experimental duration of *in* situ brain perfusion (90 s) than bBMEC studies (30 min). The lack of brain Mn influx inhibition by Ni may be due to Ni's inability to block Ca influx. The animal data, therefore, do not reveal any information whether Mn and Ca share the same BBB carrier(s) that are inhibited by Ni.

Ni significantly inhibited choroid plexus Mn influx; however, it did not inhibit Ca influx into the choroid plexus. This suggests that Mn and Ca may have separate uptake mechanisms at this blood-cerebrospinal fluid interface. The choroid plexus is believed to be the main site of Ca influx into brain. If the choroid plexus is vital in maintaining Ca homeostasis as implicated (Murphy *et al.*, 1989; Keep *et al.*, 1999), then perhaps the carriers expressed at the choroid plexus have a stronger affinity for Ca, rendering the Ni treatment an ineffective inhibitor of Ca influx. Alternatively, Ni may not have had sufficient time to inhibit Ca transporters, or the inhibition of Mn uptake into choroid plexus is independent of Ca transporters.

The results with the Ca transporter blocker, La^{3+}, suggest that a non-Ca pathway also mediates brain Mn influx. La^{3+} inhibition of Ca uptake has been shown in voltage-gated Ca channels, receptor-operated Ca channels and store-operated Ca channels (Cui and Dannies, 1992; Davidson and Guo, 2000; Liu and Ambudkar, 2001; Wu *et al.*, 2001). In perfusion studies, La^{3+} significantly increased Mn influx more than 4-fold. A literature search did not reveal any other reports of La^{3+} increasing transporter or carrier activity. There was no effect on brain Ca influx in the present studies, suggesting La^{3+} did not block Ca influx. Furthermore, the results suggest that the La^{3+} effect on Mn influx at the BBB is independent of Ca. In bBMEC studies, La^{3+} did not significantly affect Mn or Ca uptake. While rat studies indicated that La^{3+} increases Mn, but not brain Ca influx, bBMEC studies suggested a non-significant decrease in Mn and Ca uptake. The results suggest that Mn uptake at the

BBB also occurs through one or more Ca-independent processes, since La^{3+} increases Mn uptake without affecting Ca.

Another explanation for the unexpected increase in Mn uptake by La^{3+} is *trans*-stimulation of the endothelial cells. This process occurs when a substrate on one side of the cell membrane increases substrate transfer from the other side. *trans*-Stimulation has been shown to play a role in the uptake of glucose into bovine mammary epithelial cells (Xiao and Cant, 2003), agmatine through the human extraneuronal monoamine transporter (Grundemann *et al.*, 2003) and sorbitol into a renal medullary cell line (Schuttert *et al.*, 2002). ^{54}Mn efflux from astrocytes was *trans*-stimulated by ^{55}Mn in the media (Aschner*, et al.*, 1992). La^{3+} may enter cells rapidly and then cause greater Mn influx through *trans*-stimulation.

In bBMEC studies, Mn entry was inhibited by vanadate (0.003 and 1 mM). Despite indications in bBMECs, addition of 1 or 10 mM vanadate to ^{54}Mn in the *in situ* brain perfusate did not decrease brain Mn influx. Ca-ATPases are found on both the luminal and abluminal surface of brain endothelial cells, which may confound our interpretation of the results (Manoonkitiwongsa *et al.*, 2000). Mn distribution into endothelial and brain cell plus extracellular fluid fractions, as measured with the capillary depletion method, was unaltered by vanadate, suggesting neither brain Mn influx nor efflux are mediated by Ca-ATPase. Although vanadate inhibited Mn uptake into bBMECs, it did not inhibit Mn influx across the BBB. *p*-Hydroxyhippuric acid, a

relatively selective Ca-ATPase inhibitor, also did not inhibit brain Mn influx, providing further evidence against a role for Ca-ATPase.

Studies with inhibitors of voltage-gated Ca channels also failed to implicate these channels in brain Mn uptake. This is not surprising, as endothelial cells are not considered excitable and would not be expected to use voltage-gated channels. On the other hand, it was recently determined that brain endothelial cells do express L-type Ca channels (Bossu *et al.*, 1992). Verapamil did not significantly decrease Mn or Ca influx. In a similar study in the absence of ^{45}Ca, verapamil and amiloride failed to alter brain ^{54}Mn influx. These results suggest brain Mn entry is not likely to occur through voltage-gated Ca channels under physiological conditions.

Thapsigargin and CPA significantly increased Mn uptake, 2.5- and 2.6-fold, respectively, consistent with the hypothesis that SOCs play a role. Thapsigargin did not significantly increase Ca uptake (P=0.07) despite the 1.4-10-fold increase in Ca uptake. Earlier reports implicated SOCs in the influx of metals across the BBB. Lead uptake into bBMECs was increased by 1.7- and 2.1-fold following treatment with CPA or thapsigargin, respectively (Kerper and Hinkle, 1997b). The pH dependence of Mn uptake is also consistent with a role for SOCs in Mn influx at the BBB. Store-operated Ca influx was inhibited by low extracellular pH in human microglia (Khoo *et al.*, 2001). These results suggest that brain Mn uptake occurs through the SOCs.

In summary, there are at least two transporters for brain Mn influx. Mn entry into brain occurs through at least one pathway that does not have a high affinity for Ca, as evidenced with the La^{3+} data. Mn influx also is likely to occur through a Ni-blocked, CPA-induced Ca pathway, which is consistent with store-operated Ca channels.

REFERENCES

Allen DD, Smith QR. Characterization of the blood-brain barrier choline transporter using the *in situ* rat brain perfusion technique. *J Neurochem* 2001; 76(4): 1032-1041

Aschner M, Aschner JL. Manganese transport across the blood-brain barrier: relationship to iron homeostasis. *Brain Res Bull* 1990; 24(6): 857-860

Aschner M, Gannon M. Manganese (Mn) transport across the rat blood-brain barrier: saturable and transferrin-dependent transport mechanisms. *Brain Res Bull* 1994; 33(3): 345-349

Aschner M, Gannon M, Kimelberg HK. Manganese uptake and efflux in cultured rat astrocytes. *J Neurochem* 1992; 58(2): 730-735

Audus KL, Ng L, Wang W, Borchardt RT. Brain microvessel endothelial cell culture systems. In: Models for Assessing Drug Absorption and Metabolism, Ronald T. Borchardt Ea, Eds., ed., New York, Plenum Press, 1996, 239-258

Baldi C, Vazquez G, Boland R. Characterization of a 1,25(OH)2-vitamin D3-responsive capacitative Ca2+ entry pathway in rat osteoblast-like cells. *J Cell Biochem* 2002; 86(4): 678-687

Bossu JL, Elhamdani A, Feltz A, Tanzi F, Aunis D, Thierse D. Voltage-gated Ca entry in isolated bovine capillary endothelial cells: evidence of a new type of BAY K 8644-sensitive channel. *Pflugers Arch* 1992; 420(2): 200-207

Bowman PD, Ennis SR, Rarey KE, Betz AL, Goldstein GW. Brain microvessel endothelial cells in tissue culture: a model for study of blood-brain barrier permeability. *Ann Neurol* 1983; 14(4): 396-402

Chandra SV, Shukla GS, Srivastava RS, Singh H, Gupta VP. An exploratory study of manganese exposure to welders. *Clin Toxicol* 1981; 18(4): 407-416

Conrad ME, Umbreit JN, Moore EG, Hainsworth LN, Porubcin M, Simovich MJ, Nakada MT, Dolan K, Garrick MD. Separate pathways for cellular uptake of ferric and ferrous iron. *Am J Physiol Gastrointest Liver Physiol* 2000; 279(4): G767-774

Couper J. On the effects of black oxide of manganese when inhaled into the lungs. *Brit Ann Med Pharm,Vital Stat Gen Sci* 1837; 1: 41-42

Crossgrove J, Yokel R. Manganese distribution across the blood-brain barrier III; The divalent metal transporter-1 is not the major mechanism mediating brain manganese uptake. *NeuroToxicol* 2004; 25(3): 451-460

Crossgrove JS, Allen DD, Bukaveckas BL, Rhineheimer SS, Yokel RA. Manganese distribution across the blood-brain barrier I. Evidence for carrier-mediated influx of manganese citrate as well as manganese and manganese transferrin. *NeuroToxicol* 2003; 24(1): 3-13

Cui ZJ, Dannies PS. Thyrotropin-releasing hormone-mediated Mn2+ entry in perifused rat anterior pituitary cells. *Biochem J* 1992; 283 (Pt 2): 507-513

Davidson RM, Guo L. Calcium channel current in rat dental pulp cells. *J Membr Biol* 2000; 178(1): 21-3

Dobrydneva Y, Blackmore P. 2-Aminoethoxydiphenyl borate directly inhibits store-operated calcium entry channels in human platelets. *Mol Pharmacol* 2001; 60(3): 541-552

Edlund GL, Halestrap AP. The kinetics of transport of lactate and pyruvate into rat hepatocytes. Evidence for the presence of a specific carrier similar to that in erythrocytes. *Biochem J* 1988; 249(1): 117-126

Fasolato C, Hoth M, Penner R. Multiple mechanisms of manganese-induced quenching of fura-2 fluorescence in rat mast cells. *Pflugers Arch* 1993; 423(3-4): 225-231

Finley JW. Manganese uptake and release by cultured human hepato-carcinoma (Hep-G2) cells. *Biol Trace Elem Res* 1998; 64(1-3): 101-118

Goddard WP, Coupland K, Smith JA, Long RG. Iron uptake by isolated human enterocyte suspensions in vitro is dependent on body iron stores and inhibited by other metal cations. *J Nutr* 1997; 127(1): 177-183

Grundemann D, Hahne C, Berkels R, Schomig E. Agmatine is efficiently transported by non-neuronal monoamine transporters extraneuronal monoamine transporter (EMT) and organic cation transporter 2 (OCT2). *J Pharmacol Exp Ther* 2003; 304(2): 810-817

Gunshin H, Mackenzie B, Berger UV, Gunshin Y, Romero MF, Boron WF, Nussberger S, Gollan JL, Hediger MA. Cloning and characterization of a mammalian proton-coupled metal-ion transporter. *Nature* 1997; 388(6641): 482-488

Huang CC, Chu NS, Lu CS, Wang JD, Tsai JL, Tzeng JL, Wolters EC, Calne DB. Chronic manganese intoxication. *Arch Neurol* 1989; 46(10): 1104-1106

Hudnell HK. Effects from environmental Mn exposures: a review of the evidence from non-occupational exposure studies. *NeuroToxicol* 1999; 20(2-3): 379-397

Iregren A. Manganese neurotoxicity in industrial exposures: proof of effects, critical exposure level, and sensitive tests. *NeuroToxicol* 1999; 20(2-3): 315-323

Jones KT, Sharpe GR. Ni2+ blocks the Ca2+ influx in human keratinocytes following a rise in extracellular Ca2+. *Exp Cell Res* 1994; 212(2): 409-413

Keen CL, Ensunsa JL, Clegg MS. Manganese metabolism in animals and humans including the toxicity of manganese. In: Manganese and its role in biological processes, Sigel A and Sigel H, ed., New York, Marcel Dekker, Inc., 2000, 89-121

Keen CL, Lönnerdal B. Toxicity of essential and beneficial metal ions. Manganese. In: Handbook of Metal-Ligand Interactions in Biological Fluids, Berthon G, ed., New York, NY, Marcel Dekker, Inc., 1995, 683-688

Keep RF, Ulanski LJ, 2nd, Xiang J, Ennis SR, Lorris Betz A. Blood-brain barrier mechanisms involved in brain calcium and potassium homeostasis. *Brain Res* 1999; 815(2): 200-205

Kerper LE, Hinkle PM. Cellular uptake of lead is activated by depletion of intracellular calcium stores. *J Biol Chem* 1997a; 272(13): 8346-8352

Kerper LE, Hinkle PM. Lead uptake in brain capillary endothelial cells: activation by calcium store depletion. *Toxicol Appl Pharmacol* 1997b; 146(1): 127-133

Khoo C, Helm J, Choi HB, Kim SU, McLarnon JG. Inhibition of store-operated Ca(2+) influx by acidic extracellular pH in cultured human microglia. *Glia* 2001; 36(1): 22-30

Kim YV, Di Cello F, Hillaire CS, Kim KS. Differential Ca^{2+} signaling by thrombin and protease-activated receptor-1-activating peptide in human brain microvascular endothelial cells. *Am J Physiol Cell Physiol* 2004; 286(1):C31-42

Klaassen CD. Biliary excretion of manganese in rats, rabbits, and dogs. *Toxicol Appl Pharmacol* 1974; 29(3): 458-468

Kondakis XG, Makris N, Leotsinidis M, Prinou M, Papapetropoulos T. Possible health effects of high manganese concentration in drinking water. *Arch Environ Health* 1989; 44(3): 175-178

Kukkonen JP, Lund PE, Akerman KE. 2-aminoethoxydiphenyl borate reveals heterogeneity in receptor-activated Ca(2+) discharge and store-operated Ca(2+) influx. *Cell Calcium* 2001; 30(2): 117-129

Lee J-W. Manganese Intoxication. *Arch Neurol* 2000; 57(4): 597-599

Liu X, Ambudkar IS. Characteristics of a store-operated calcium-permeable channel: sarcoendoplasmic reticulum calcium pump function controls channel gating. *J Biol Chem* 2001; 276(32): 29891-29898

Lockman PR, Roder KE, Allen DD. Inhibition of the rat blood-brain barrier choline transporter by manganese chloride. *J Neurochem* 2001; 79(3): 588-594

Manoonkitiwongsa PS, Whitter EF, Wareesangtip W, McMillan PJ, Nava PB, Schultz RL. Calcium-dependent ATPase unlike ecto-ATPase is located primarily on

the luminal surface of brain endothelial cells. *Histochem J* 2000; 32(5): 313-24

Mason MJ, Mayer B, Hymel LJ. Inhibition of Ca2+ transport pathways in thymic lymphocytes by econazole, miconazole, and SKF 96365. *Am J Physiol* 1993; 264(3 Pt 1): C654-662

Murphy VA, Smith QR, Rapoport SI. Uptake and concentrations of calcium in rat choroid plexus during chronic hypo- and hypercalcemia. *Brain Res* 1989; 484(1-2): 65-70

Murphy VA, Wadhwani KC, Smith QR, Rapoport SI. Saturable transport of manganese(II) across the rat blood-brain barrier. *J Neurochem* 1991; 57(3): 948-954

Ono K, Komai K, Yamada M. Myoclonic involuntary movement associated with chronic manganese poisoning. *J Neurol Sci* 2002; 199(1-2): 93-96

Poole RC, Halestrap AP, Price SJ, Levi AJ. The kinetics of transport of lactate and pyruvate into isolated cardiac myocytes from guinea pig. Kinetic evidence for the presence of a carrier distinct from that in erythrocytes and hepatocytes. *Biochem J* 1989; 264(2): 409-418

Rabin O, Hegedus L, Bourre JM, Smith QR. Rapid brain uptake of manganese (II) across the blood-brain barrier. *J Neurochem* 1993; 61: 509-517

Schuttert JB, Fiedler GM, Grupp C, Blaschke S, Grunewald RW. Sorbitol transport in rat renal inner medullary interstitial cells. *Kidney Int* 2002; 61(4): 1407-1415

Shibuya I, Douglas WW. Calcium channels in rat melanotrophs are permeable to manganese, cobalt, cadmium, and lanthanum, but not to nickel: evidence

provided by fluorescence changes in fura-2-loaded cells. *Endocrinol* 1992; 131(4): 1936-1941

Wedler FC, Denman RB. Glutamine synthetase: the major Mn(II) enzyme in mammalian brain. *Curr Top Cell Reg* 1984; 24: 153-169

Wu S, Sangerman J, Li M, Brough GH, Goodman SR, Stevens T. Essential control of an endothelial cell ISOC by the spectrin membrane skeleton. *J Cell Biol* 2001; 154(6): 1225-1233

Xiao C, Cant JP. The glucose transporter in bovine mammary epithelial cells is an asymmetric carrier that exhibits cooperativity and trans-stimulation. *Am J Physiol Cell Physiol* 2003; 285(5): C1226-1234

Yamakami J, Sakurai E, Sakurada T, Maeda K, Hikichi N. Stereoselective blood-brain barrier transport of histidine in rats. *Brain Res* 1998; 812(1-2): 105-112

Yokel R, Wilson M, Harris W, Halestrap A. Aluminum citrate uptake by immortalized brain endothelial cells: Implications for its blood-brain barrier transport. *Brain Res* 2002; 930(1-2): 101-110

Yokel RA, Crossgrove JS, Bukaveckas BL. Manganese distribution across the blood-brain barrier II. Manganese efflux from the brain does not appear to be carrier mediated. *NeuroToxicol* 2003; 24(1): 15-22

Table 1. Characteristics of $^{54}Mn^{2+}$ uptake into bBMECs

Treatment	Mn uptake (% control ± SEM)	n
Control (122 mM Na^+)	100 ± 7	6
61 mM Na^+, 61 mM choline	97 ± 18	3
122 mM% Choline (no Na^+)	160 ± 6*	5
122 mM Li^+ (no Na^+)	90 ± 9	4
Control (vehicle)	100 ± 10	3
Ouabain	129 ± 15	3
Control (vehicle)	100 ± 6	8
2,4-Dinitrophenol	102 ± 5	6
Azide	124 ± 4	3
2-Deoxyglucose	84 ± 8	4

* = significantly different from control.

Table 2. Mn and Ca uptake into bBMECs in the presence of Ca transporter inhibitors

Treatment	Ca uptake (% control ± SEM)	Mn uptake (% control ± SEM)	N
Control		100 ± 18	5
No Ca^{2+}		170 ± 29*	4
Control		100 ± 5	4
Vanadate (0.003 μM)		64 ± 3*	3
Vanadate (1 mM)		53 ± 4*	3
Vanadate pretreatment (1 mM)		39 ± 4*	3
Control	100 ± 17	100 ± 8	4
La^{3+}	58 ± 25*	64 ± 24	4
Ni^{2+}	15 ± 15*	12 ± 3*	3
Verapamil	54 ± 3	81 ± 2	3
Control (vehicle)	100 ± 30	100 ± 13	3
CPA	418 ± 98*	265 ± 48*	4
Thapsigargin	415 ± 212	252 ± 23*	4

* =significantly different from control.

Figure 1. Mn uptake into bBMECs correlates inversely with proton concentration. Values are mean percent of control (pH 7.4) uptake ± SEM for 3-6 experiments, following 30 minute incubation. *Inset*: Time dependent uptake of Mn at pH 6.4 versus 7.4 is shown. * denotes a significant difference from control

Figure 2. The Arrhenius plot shows temperature-dependent Mn uptake into bBMECs. Values shown are the natural log of the mean ± SEM of uptake (pmol/30 min/mg).

Figure 3. Mn influx correlates negatively with Ca concentration following *in situ* perfusion, but Mn concentration has no effect on Ca influx. A) Mn and B) Ca influx values into brain are shown (mean ± SEM of 4-5 animals).

Figure 4. La increased Mn influx into rat brain. Values shown are mean ± SEM (n=5). The Y-axis in panel A is different from previous Mn influx graphs.

Figure 5. Ni did not decrease Mn (A) influx into rat brain across the BBB. Values shown are mean ± SEM (n=5). * significantly different from control

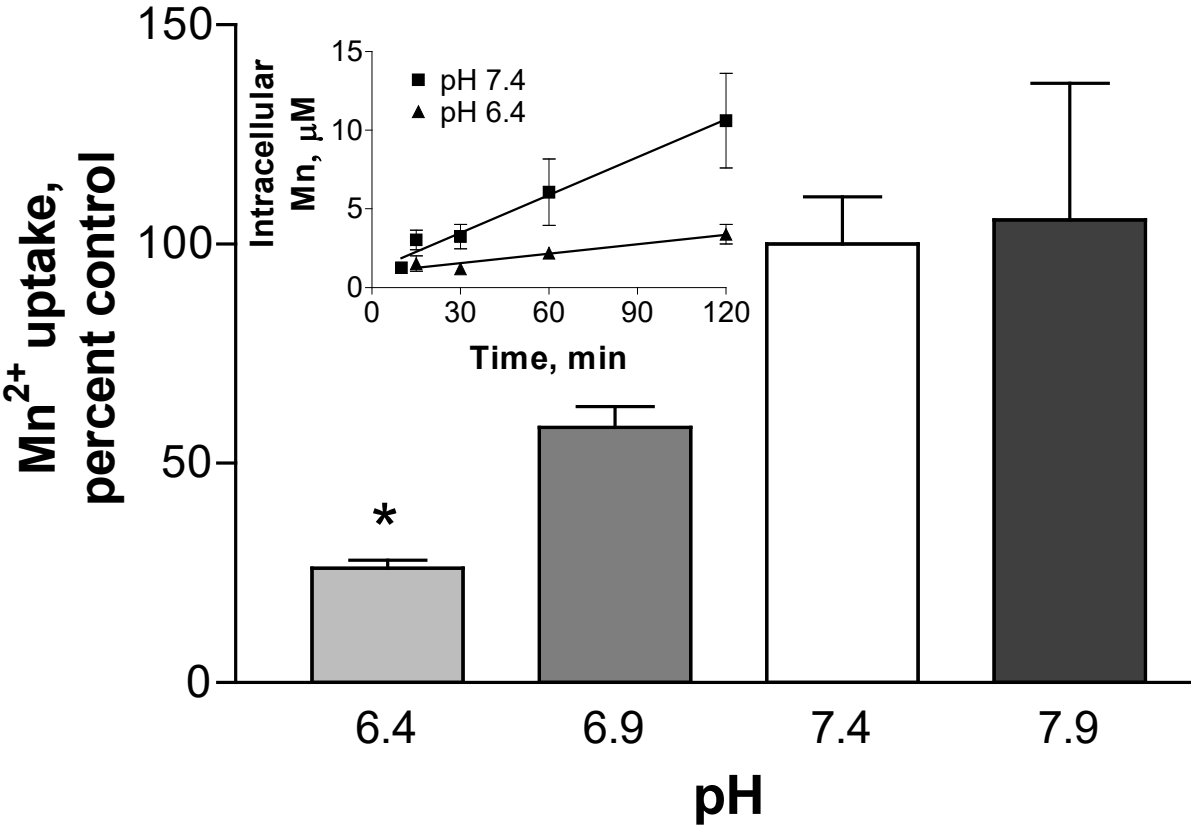
150
100
50
0
Mn^{2+} uptake, percent control
*
6.4
6.9
7.4
7.9
pH
Intracellular Mn, μM
15
10
5
0
pH 7.4
pH 6.4
0
30
60
90
120
Time, min

Figure 1

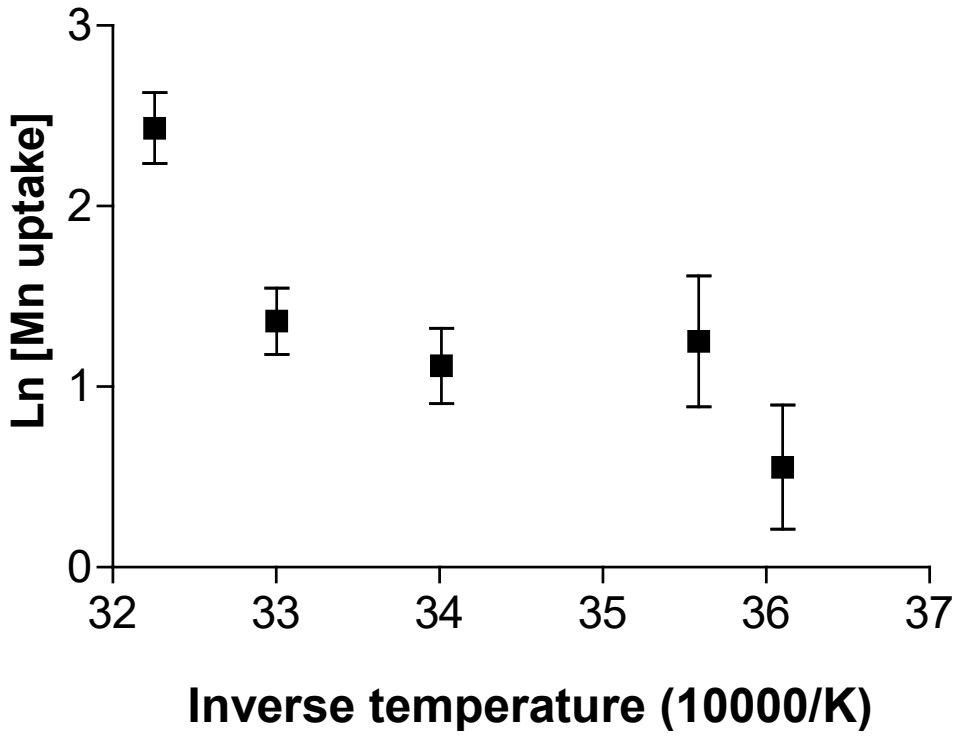
Ln [Mn uptake]
3
2
1
0
32
33
34
35
36
37
Inverse temperature (10000/K)

Figure 2

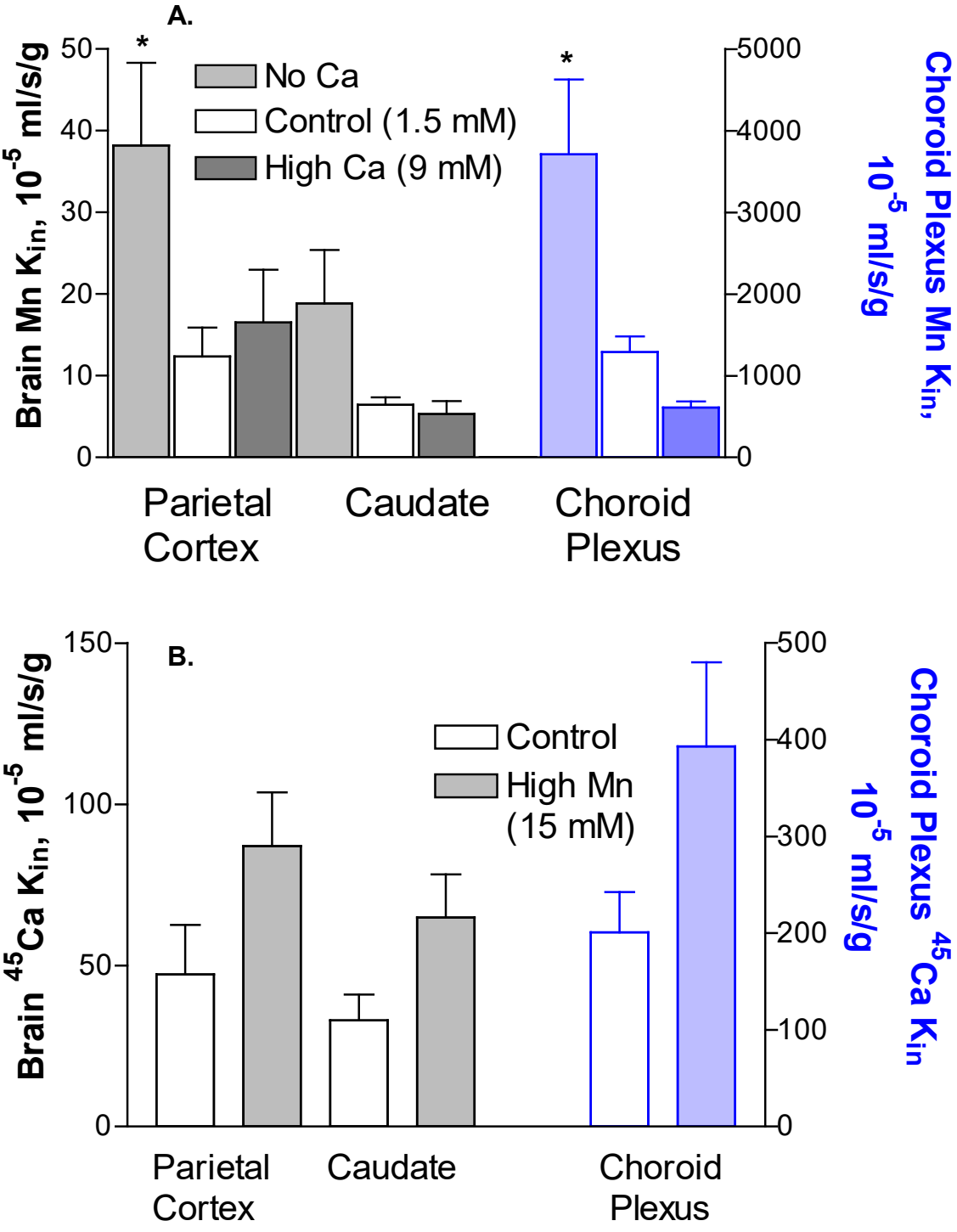
A.
Brain Mn K_{in}, 10^{-5} ml/s/g
Choroid Plexus Mn K_{in}, 10^{-5} ml/s/g
No Ca
Control (1.5 mM)
High Ca (9 mM)
*
*
0
10
20
30
40
50
0
1000
2000
3000
4000
5000
Parietal Cortex
Caudate
Choroid Plexus
B.
Brain ^{45}Ca K_{in}, 10^{-5} ml/s/g
Choroid Plexus ^{45}Ca K_{in} 10^{-5} ml/s/g
Control
High Mn (15 mM)
0
50
100
150
0
100
200
300
400
500
Parietal Cortex
Caudate
Choroid Plexus

Figure 3

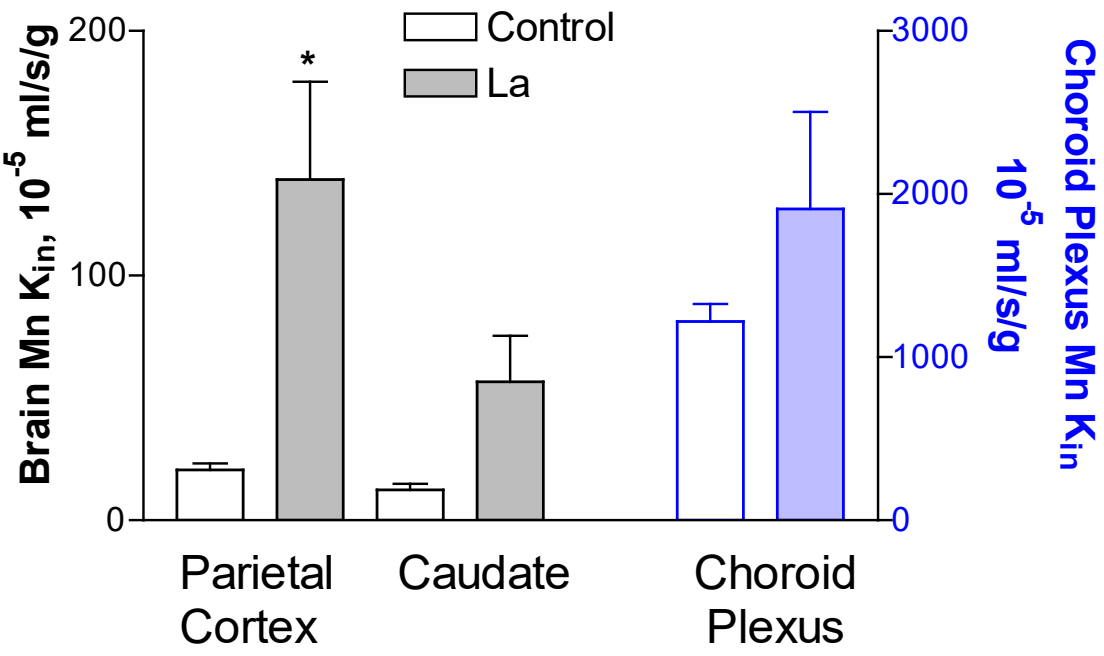
Brain Mn K_{in}, 10^{-5} ml/s/g
200
100
0
*
Control
La
3000
2000
1000
0
Choroid Plexus Mn K_{in}
10^{-5} ml/s/g
Parietal Cortex
Caudate
Choroid Plexus

Figure 4

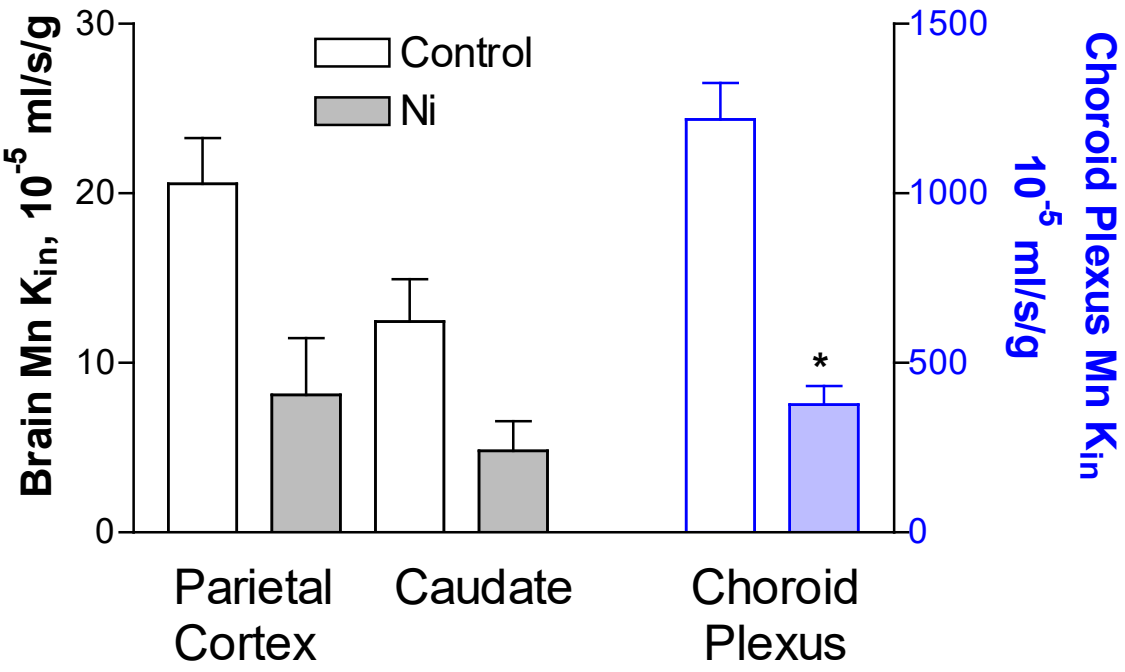
Brain Mn K_{in}, 10^{-5} ml/s/g
30
20
10
0
Control
Ni
1500
1000
500
0
Choroid Plexus Mn K_{in}
10^{-5} ml/s/g
*
Parietal Cortex
Caudate
Choroid Plexus

Figure 5